2,2´-Tethered Binaphthyl-Embedded One-Handed Helical Ladder Polymers: Impact of the Tether Length on Helical Geometry and Chiroptical Property

Tomoyuki Ikai,*[a],[b] Namiki Mishima,[a] Takehiro Matsumoto,[a] Sayaka Miyoshi,[a] Kosuke Oki,[a] and Eiji Yashima[a]

[a] Dr. T. Ikai, N. Mishima, T. Matsumoto, S. Miyoshi, Dr. K. Oki, Prof. E. Yashima
Department of Molecular and Macromolecular Chemistry
Graduate School of Engineering, Nagoya University
Chikusa-ku, Nagoya 464-8603 (Japan)
E-mail: ikai@chembio.nagoya-u.ac.jp; yashima@chembio.nagoya-u.ac.jp

[b] Dr. T. Ikai
Precursory Research for Embryonic Science and Technology (PRESTO)
Japan Science and Technology Agency (JST)
Kawaguchi, Saitama 332-0012 (Japan)

Supporting information for this article is given via a link at the end of the document.

Abstract: Synthetic breakthroughs diversify the molecules and polymers available to chemists. We now report the first successful synthesis of a series of optically-pure 2,2´-tethered binaphthyl-embedded helical ladder polymers based on quantitative and chemoselective ladderization by the modified alkyne benzannulations using the 4-alkoxy-2,6-dimethylphenylethynyl group as the alkyne source, inaccessible by the conventional approach lacking the 2,6-dimethyl substituents. Due to the defect-free helix formation, the circular dichroism signal increased by more than 6 times the previously reported value. The resulting helical secondary structure can be fine-tuned by controlling the binaphthyl dihedral angle in the repeating unit with variations in the 2,2´-alkylenedioxy tethering groups by one carbon atom at a time. The optimization of the helical ladder structures led to a strong circularly polarized luminescence with a high fluorescence quantum yield (28%) and luminescence dissymmetry factor (2.6×10^{-3}).

Introduction

Material properties ultimately rely on the structures of the (macro)molecules that they contain. Therefore, not only the precise design of molecules and polymers, but also the advanced synthetic methodology capable of producing them are necessary for the development of high value-added materials with excellent physical properties and/or sophisticated functions.

The one-handed twisted axially chiral 1,1´-binaphthyl[1] is one of the most representative optically-active frameworks widely incorporated into chiral functional materials for asymmetric catalysis,[2] chiral recognition,[3] and circularly polarized luminescence[4] as well as chiral dopants to induce chiral nematic liquid crystals.[5] The optical and chiroptical properties and functionalities of the 1,1´-binaphthyl compounds are highly dependent on the dihedral angle between the two naphthalene rings.[6] Typical 1,1´-binaphthyl compounds with independent substituents at the 2,2´-positions have a static axial chirality, yet possess a considerable conformational freedom, thus their properties and functional capabilities vary with rotation around the biaryl axis, making the precise and target-oriented molecular design difficult.[4a,7] The binaphthyl dihedral angle can be fixed and arbitrarily controlled by tethering at the 2,2´-positions with an appropriate spacer.[8] A variety of molecules[9] and polymers[7b,10] containing shape-persistent 2,2´-tethered binaphthyl units has been reported, in which the chiroptical properties,[11] asymmetric catalytic activities,[12] and helical twisting powers of the chiral dopants[5a,13] have been modulated by tuning the binaphthyl dihedral angle through simple replacement of the tethering groups. Pu and a co-worker designed a random-coil precursor polymer (poly-**4R^{C1}**-H in Figure 1a) containing an optically-pure 2,2´-methylenedioxy-tethered binaphthyl moiety in the main chain[14] and attempted to convert it into a ladder polymer[15] with a one-handed helical structure (helical ladder polymer) by ladderization of the entire backbone through the conventional acid-promoted alkyne benzannulations, in which the *ortho*-unsubstituted 4-alkoxyphenylethynyl pendants were introduced into the precursor polymers as alkyne sources.[16] However, due to the low chemoselectivity of this conventional approach, the resulting polymer (poly-**5R^{C1}**-H) had an irregular backbone structure composed of different repeating units (Figure 1a),[17] precluding the formation of the desired one-handed helical ladder structure.[14]

We recently succeeded in significantly improving the chemoselectivity of the alkyne benzannulation by introducing methyl groups at the 2,6-positions of the 4-alkoxyphenyl pendants in order to enhance the steric effect.[18] This modified approach allowed the synthesis of defect-free one-handed helical ladder polymers with tubular[19] and ribbon[18,19b] geometries (Figure 1b). To date, chiral units incorporated into the helical ladder backbones to control the helical geometry and handedness (right (*P*)- and left (*M*)-handed) were limited to the optically-pure 2,6-linked-triptycene[17,19b] and 4,4´- and 6,6´-linked-1,1´-spirobiindane[18-19] units (Figure 1b). In order to diversify the helical frameworks and explore the unique functions characteristic of their structures,[20] the expansion of chiral substrates applicable to the quantitative and chemoselective modified alkyne benzannulation is highly required.

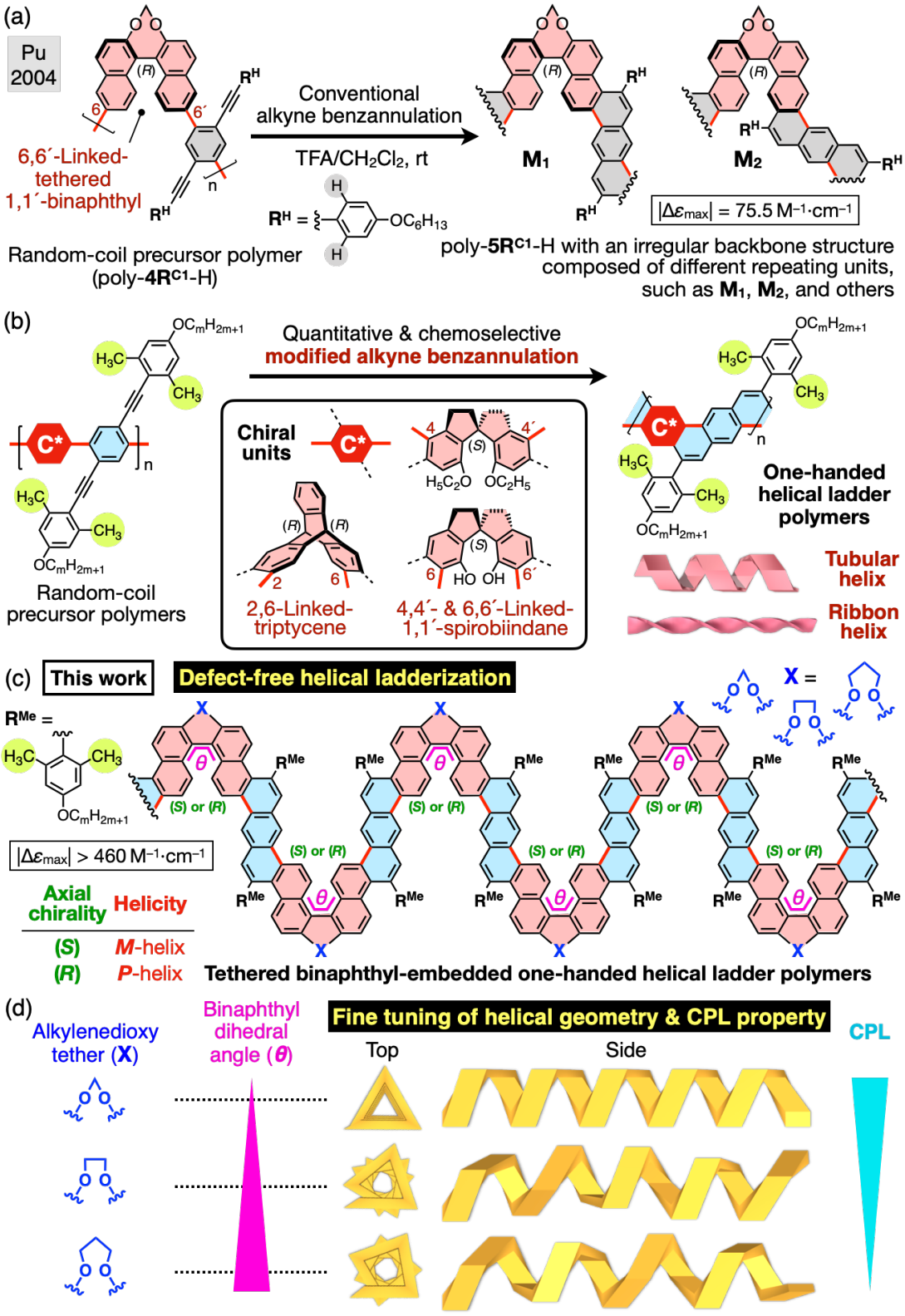

Figure 1. (a) Conventional alkyne benzannulation of a random-coil precursor polymer (poly-**4R**^{C1}-H) containing a 6,6´-linked-tethered 1,1´-binaphthyl unit to provide an irregular ladder polymer (poly-**5R**^{C1}-H) with a relatively weak circular dichroism (CD) (the maximum molar CD ($|\Delta\varepsilon_{max}|$) = 75.5 $M^{-1}\cdot cm^{-1}$). (b) Synthesis of tubular- and ribbon-shaped helical ladder polymers containing optically-pure 2,6-linked-triptycene and 4,4´- and 6,6´-linked-1,1´-spirobiindane units by quantitative and chemoselective modified alkyne benzannulations. (c) Structure of the defect-free tethered binaphthyl-embedded one-handed helical ladder polymers with different alkylenedioxy tethers showing $|\Delta\varepsilon_{max}|$ greater than 460 $M^{-1}\cdot cm^{-1}$. (d) Schematic illustration of fine tuning of the helical geometry and circularly polarized luminescence (CPL) property based on the control of the binaphthyl dihedral angle by changing the alkylenedioxy tethers.

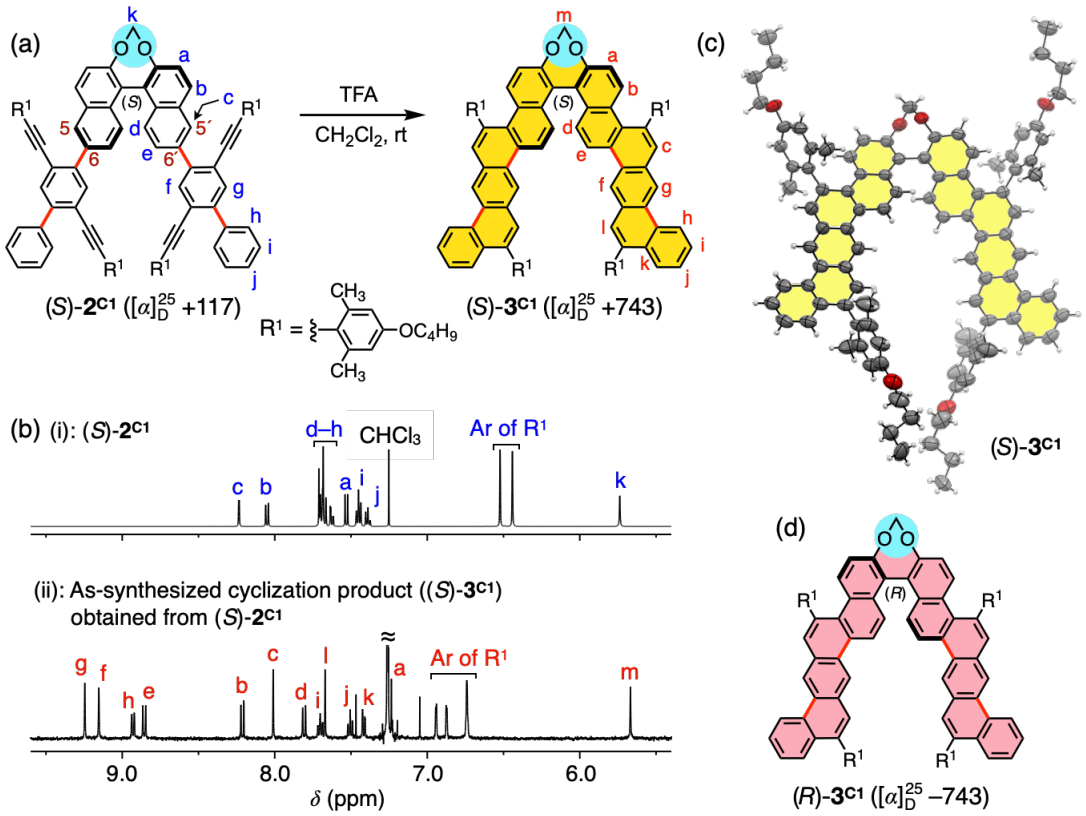

Figure 2. (a) Synthesis of an optically-pure methylenedioxy-tethered (*S*)-1,1´-binaphthyl-bound ladder-type molecule ((*S*)-**3**^{C1}) through quantitative and chemoselective modified alkyne benzannulation of (*S*)-**2**^{C1}. (b) ^{1}H NMR spectra (500 MHz, $CDCl_3$, 25 °C) of (*S*)-**2**^{C1} (i) and an as-synthesized cyclization product ((*S*)-**3**^{C1}) obtained from (*S*)-**2**^{C1} (ii). For the signal assignments and the corresponding IR spectra, see Figures S2–S4. (c) X-ray crystal structure of (*S*)-**3**^{C1}. (d) Structure of (*R*)-**3**^{C1}.

We envisioned that if the modified alkyne benzannulation could be applied to the 6,6´-linked-1,1´-binaphthyl framework, we could realize the defect-free synthesis of the 2,2´-tethered binaphthyl-embedded helical ladder polymer that was inaccessible by the conventional approach.[14,16] In addition, the precise modulation of the resulting helical structures would also be possible based on the rational control of the binaphthyl dihedral angle by changing the tether structure at the 2,2´-positions of the 1,1´-binaphthyl unit. We now report the successful synthesis of a novel series of defect-free one-handed helical ladder polymers containing one-handed twisted 2,2´-tethered binaphthyl units with different tether lengths through the modified alkyne benzannulations (Figure 1c).[18] We further investigated the fine-tuning of the helical structure by controlling the one-handed twist angle of the 1,1´-binaphthyl unit with variations in the 2,2´-alkylenedioxy tethers (Figure 1d), taking full advantage of the completely interconnected rigid ladder structure, in which a slight difference in the primary structures directly leads to the secondary structural change. The impact of the defect-free ladderization and the resulting helical geometries on the circular dichroism (CD) and circularly polarized luminescence (CPL) properties is also highlighted.

Results and Discussion

Defect-Free Synthesis of 2,2´-Tethered Binaphthyl-Embedded One-Handed Helical Ladder Polymers

We first investigated the feasibility of the quantitative and chemoselective π-extension of the 2,2´-tethered binaphthyl framework through the modified alkyne benzannulation. Optically-pure 2,2´-methylenedioxy-tethered 1,1´-binaphthyl derivatives ((*S*)- and (*R*)-**2**^{C1}) carrying 4-phenyl-2,5-bis[2-(4-alkoxy-2,6-dimethylphenyl)ethynyl]phenyl groups at the 6,6´-positions of the binaphthyl moiety were synthesized as cyclization model precursors (Scheme S1), then subjected to the modified acid-promoted alkyne benzannulations in a dichloromethane/trifluoroacetic acid (TFA) mixture according to a previously reported method (Figure 2a and Scheme S1).[18-19] The cyclizations of (*S*)- and (*R*)-**2**^{C1} regioselectively proceeded only at the 5,5´-positions of the 1,1´-binaphthyl moiety, quantitatively yielding (*S*)- and (*R*)-**3**^{C1} as single ladderization products within 1 h, respectively (Figure 2a,b,d), as confirmed by IR (Figure S2b,d), 1D and 2D NMR (Figures 2b(ii) and S4), high-resolution mass (section 2 in the Supporting Information (SI)), and single-crystal X-ray crystallography (Figures 2c and S1) analyses. This result is in sharp contrast to the conventional alkyne benzannulation of the analogous cyclization precursor ((*R*)-**2**^{C1}-H in Figure S5) lacking the 2,6-dimethyl substituents on the 4-alkoxyphenyl pendants, which gave a complicated product mixture,[17] demonstrating that the modified alkyne benzannulation can be successfully applied to the 6,6´-linked-1,1´-binaphthyl moiety.

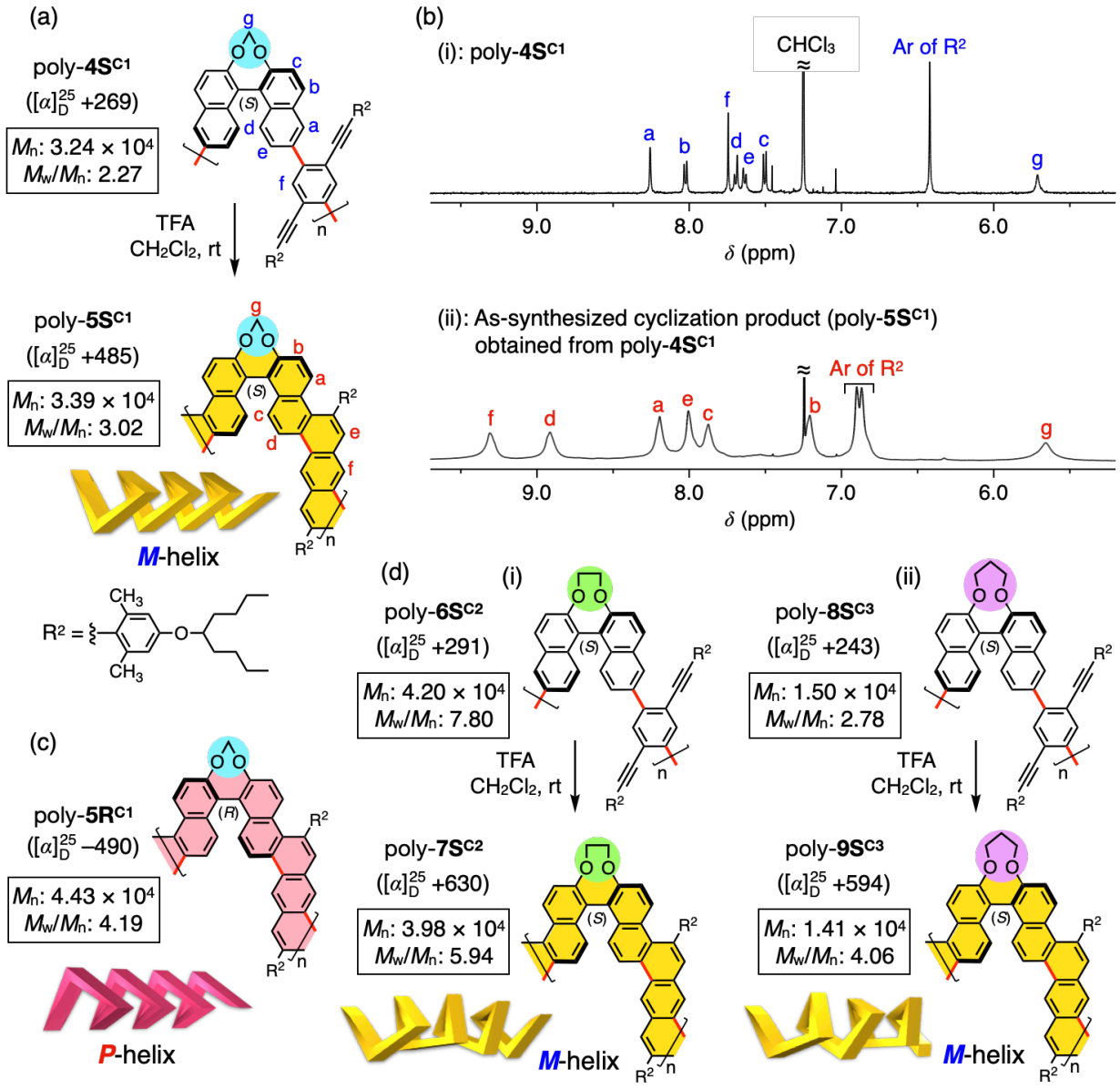

Figure 3. (a) Synthesis of a methylenedioxy-tethered (*S*)-1,1´-binaphthyl-bound (*M*)-handed helical ladder polymer (poly-**5S**^{C1}) by quantitative and chemoselective modified alkyne benzannulations of poly-**4S**^{C1}. (b) ^{1}H NMR spectra (500 MHz, $CDCl_3$, 50 °C) of poly-**4S**^{C1} (i) and poly-**5S**^{C1} (ii). For the signal assignments, see Figures S6 and S7, respectively. (c) Structure of poly-**5R**^{C1}. (d) Synthesis of ethylenedioxy- (i) and propylenedioxy- (ii) tethered (*S*)-1,1´-binaphthyl-bound (*M*)-handed helical ladder polymers (poly-**7S**^{C2} and poly-**9S**^{C3}) by quantitative and chemoselective modified alkyne benzannulations of poly-**6S**^{C2} and poly-**8S**^{C3}, respectively.

Based on this finding, we then investigated the defect-free synthesis of the 2,2´-tethered binaphthyl-embedded one-handed helical ladder polymers (Figure 1c). The Suzuki-Miyaura coupling copolymerizations of the optically-pure 1,1´-binaphthyl-based diboronic acid ester monomers ((*S*)- and (*R*)-**1Me**) with a *p*-dibromobenzene derivative (Ph-Br_2) provided the precursor polymers (poly-**4S**^{C1} and poly-**4R**^{C1}) (Scheme S2) with the number-average molar mass (M_n) and degree of polymerization (DP_n) of more than 3.24×10^4 and 35, respectively, as estimated by size-exclusion chromatography (SEC) (entries 1 and 2 in Table S1). The modified alkyne benzannulations of poly-**4S**^{C1} and poly-**4R**^{C1} gave the ladder polymers, poly-**5S**^{C1} and poly-**5R**^{C1}, respectively (Figure 3a,c and Scheme S3), showing a new single set of well-resolved resonance peaks in the ^{1}H NMR spectra (Figure 3b(ii)), all of which could be unambiguously assigned by the 2D NMR analysis (Figure S7). The matrix-assisted laser desorption-ionization time-of-flight mass (MALDI-TOF-MS) spectrum of poly-**5S**^{C1} showed a main series of peaks with distances of approximately 913 Da corresponding to the molar mass of the repeating unit (Figure S12b). These results indicated that the intramolecular cyclizations of poly-**4S**^{C1} and poly-**4R**^{C1} proceeded in a completely chemoselective manner as observed for (*S*)- and (*R*)-**2**^{C1}, affording the quantitative formation of the defect-free one-handed helical ladder polymers, poly-**5S**^{C1} and poly-**5R**^{C1}, respectively. Analogous defect-free helical ladder polymers, poly-**7S**^{C2} and poly-**9S**^{C3}, with the longer ethylenedioxy and propylenedioxy tethers, respectively, at the 2,2´-positions of

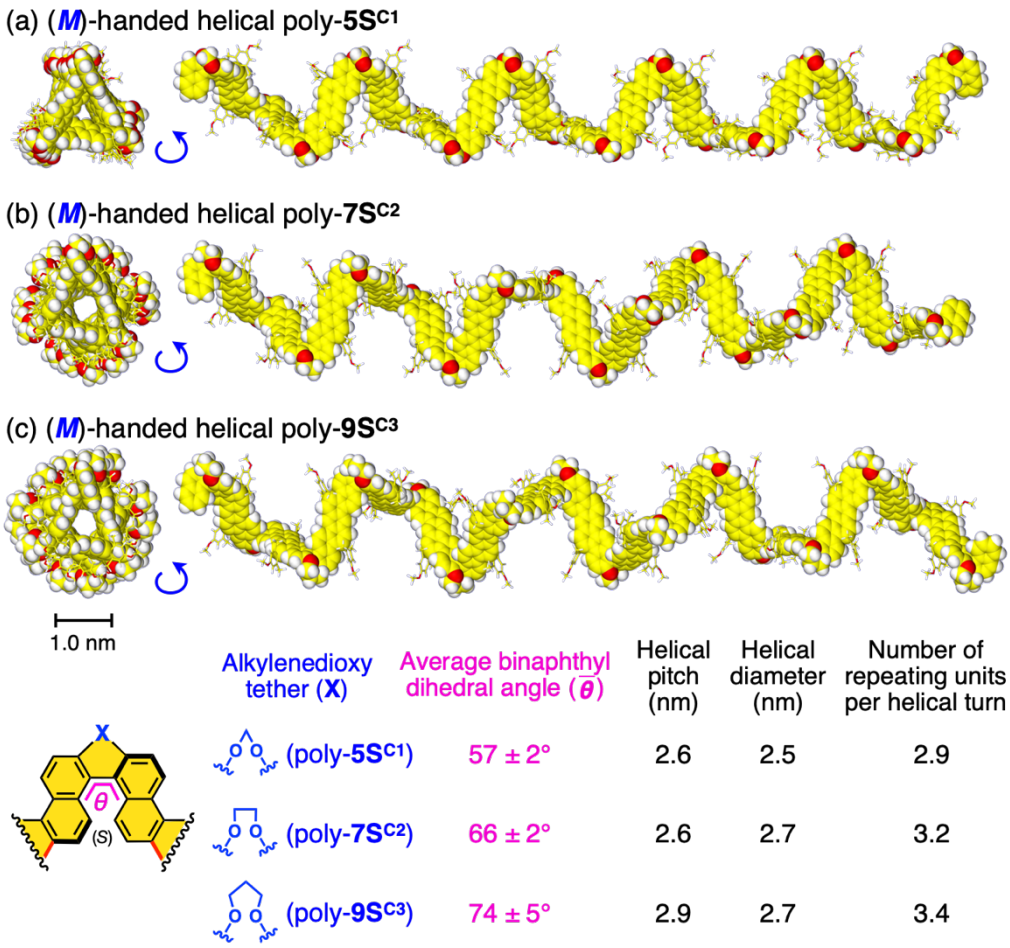

Figure 4. Top (left) and side (right) views of the geometry-optimized structures of (*M*)-handed helical poly-**5S**^{C1} (a), poly-**7S**^{C2} (b), and poly-**9S**^{C3} (c) with 15 repeating units obtained by the molecular mechanics calculations (Compass II force field). For simplicity, all alkoxy pendants are replaced with methoxy groups. The structures of the helical ladder backbones and alkoxyphenyl pendants are represented by space-filling and capped-stick models, respectively, and the carbon atoms of the helical ladder backbones are highlighted in yellow for clarity. The average binaphthyl dihedral angle ($\bar{\theta}$), helical pitch and diameter, and number of repeating units per helical turn of each helical ladder polymer are also shown.

the 1,1´-binaphthyl units were also synthesized from the corresponding precursor polymers, poly-**6S**^{C2} and poly-**8S**^{C3} (entries 3 and 4 in Table S1), by the modified alkyne benzannulations (Figures 3d and S13a,b; for the corresponding IR, 2D NMR, and MALDI-TOF-MS spectra, see Figures S2j,l, S9, S11, and S12c,d).

Fine-Tuning of Helical Geometry Based on the Control of Binaphthyl Dihedral Angles by Changing Alkylenedioxy Tethers

Possible helical ladder structures (15-mer) of a series of (*S*)-1,1´-binaphthyl-embedded poly-**5S**^{C1}, poly-**7S**^{C2}, and poly-**9S**^{C3} with different 2,2´-alkylenedioxy tethers optimized by molecular mechanics calculations are shown in Figure 4. The average binaphthyl dihedral angles ($\bar{\theta}$ in Figure 4) of poly-**5S**^{C1}, poly-**7S**^{C2}, and poly-**9S**^{C3} increase with the tether length and are found to be ca. 57°, 66°, and 74°, respectively, which are roughly comparable to those of the recently reported 2,2´-alkylenedioxy-tethered 1,1´-binaphthyl derivatives.[10c,11d,e,13f] All three ladder polymers have an (*M*)-handed macromolecular helicity due to the same axial chirality of the (*S*)-1,1´-binaphthyl moieties, but differ in the helical geometries, including the helical pitch (2.6 – 2.9 nm), helical diameter (2.5 – 2.7 nm), and the number of repeating units per helical turn (2.9 – 3.4) as well as the groove structure. These results indicated that the systematic structural variation of the repeating units based on the simple replacement of the tethering groups allowed fine-tuning of the secondary structures, while maintaining the binaphthyl (*S*)-axial chirality (Figure 1d).

Chiroptical Properties of Helical Ladder Polymers with Precisely Modulated Secondary Structures

The enantiomeric (*M*)- and (*P*)-handed helical poly-**5S**^{C1} and poly-**5R**^{C1}, respectively, showed intense mirror-image CD signals in chloroform in the main-chain absorption regions (Figure 5a(ii,iv)), in contrast to the precursor polymers with very weak CDs (Figure 5a(i,iii)). The maximum molar CD intensity at 336 nm of poly-**5**^{C1} ($|\Delta\varepsilon_{max}| \geq 460$; Figure 5a(ii,iv)) is more than 6-fold

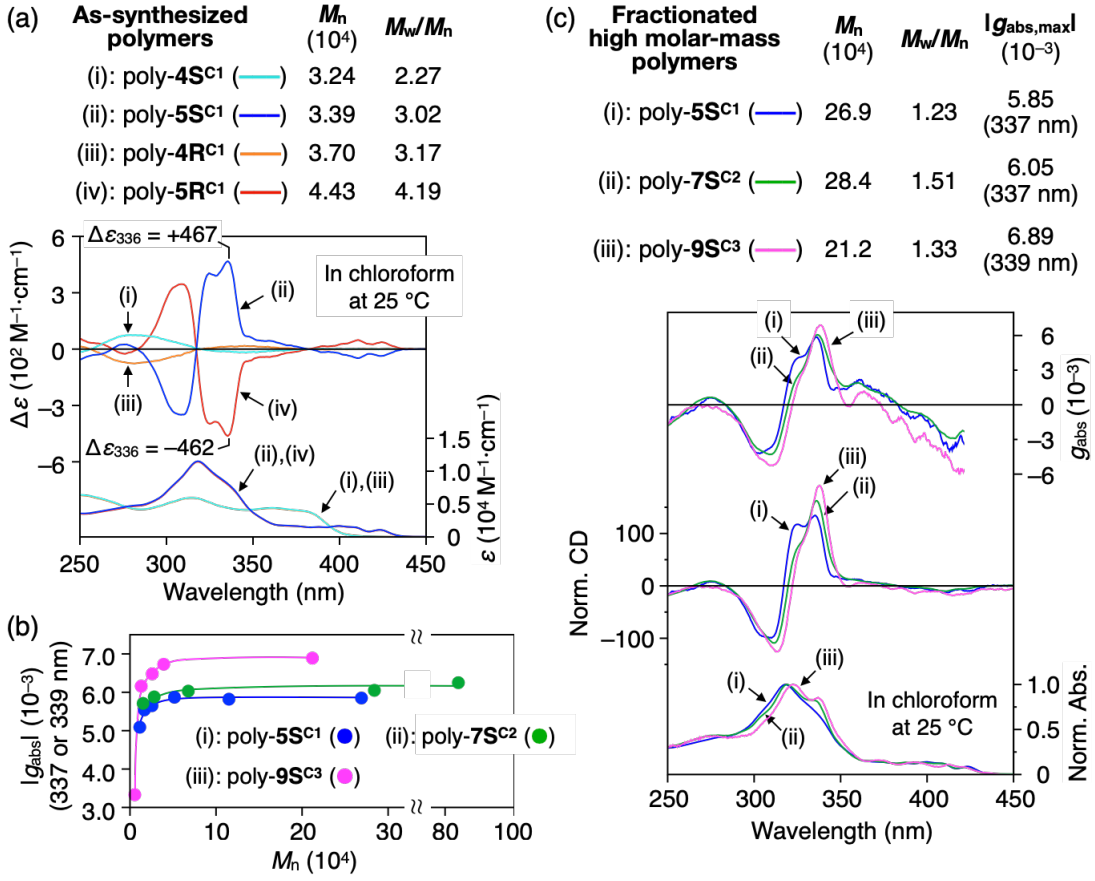

Figure 5. (a) CD and absorption spectra of poly-**4S^{C1}** (i), poly-**5S^{C1}** (ii), poly-**4R^{C1}** (iii), and poly-**5R^{C1}** (iv) in chloroform at 25 °C. [Repeating units of polymer] = 0.10 mM. (b) Plots of Kuhn's dissymmetry factors ($|g_{abs}|$) at the first Cotton effect (337 (i,ii) or 339 (iii) nm) of poly-**5S^{C1}** (i), poly-**7S^{C2}** (ii), and poly-**9S^{C3}** (iii) versus the M_n value. For the SEC fractionation and the corresponding CD spectra, see b and c in Figures S15–S17. (c) Absorption (bottom), CD (middle), and g_{abs} (top) spectra of fractionated high molar-mass poly-**5S^{C1}** (i; **f1** in Figure S15b), poly-**7S^{C2}** (ii; **f2** in Figure S16b), and poly-**9S^{C3}** (iii; **f1** in Figure S17b) (M_n > 20 × 10^4) measured in chloroform at 25 °C after SEC fractionation. The CD and absorption spectra were normalized based on the corresponding absorption spectra at 25 °C.

higher than the value reported for the 2,6-dimethyl-lacking analogue, poly-**5R^{C1}**-H ($|\Delta\varepsilon_{max}|$ = 75.5; Figure 1a), synthesized by the classical alkyne benzannulations.[14] Because the CD spectral patterns and intensities of poly-**5S^{C1}** were virtually independent of the polymer concentration (Figure S14a), its strong CD signal was due to the macromolecular helicity and not due to the supramolecular chirality resulting from the chiral self-assembly. Therefore, we can confidently state that the remarkable chiroptical enhancement of poly-**5S^{C1}** and poly-**5R^{C1}** compared to poly-**5R^{C1}**-H is obviously due to their defect-free helical ladder structures by the modified alkyne benzannulations. In addition, the maximum Kuhn's dissymmetry factor ($|g_{abs}| = |\Delta\varepsilon/\varepsilon|$) of poly-**5S^{C1}** tended to increase with the increasing molar mass (Figures 5b(i) and S15b,c) probably due to the negligible end-group effect, reaching the almost constant value ($|g_{abs}|$ = ca. 5.8 × 10^{-3}) at the M_n of more than ca. 5 × 10^4 (corresponding to ca. > 55 repeating units) (Figure 5b(i)), which is slightly higher than that of (*S*)-**3^{C1}** ($|g_{abs}|$ = ca. 5.3 × 10^{-3}) (Figure S18a(ii)).

The as-synthesized poly-**7S^{C2}** and poly-**9S^{C3}** also showed much stronger CD signals than their precursors as a result of the helical ladder formations (Figure S13c). When compared among the fractionated polymers with sufficiently high molecular masses (M_n > 20 × 10^4) (b and c in Figures S15–S17), the CD and absorption intensities and patterns of poly-**5S^{C1}**, poly-**7S^{C2}**, and poly-**9S^{C3}** were similar but slightly different from each other (Figure 5b,c), which was attributed to the variations in the helical structures and π-conjugation lengths induced by the tether length-dependent change in the binaphthyl dihedral angles. The maximum $|g_{abs}|$ values at the intense Cotton effect around 340 nm increased with an increase in the tether length in the following order: poly-**5S^{C1}** (5.85 × 10^{-3}) < poly-**7S^{C2}** (6.05 × 10^{-3}) < poly-**9S^{C3}** (6.89 × 10^{-3}) (Figure 5c). The $|g_{abs}|$ values of all the helical ladder polymers hardly changed in the temperature range of 25 – 80 °C in 1,1,2,2-tetrachloroethane (Figure S19), indicating the thermally-stable helical structures derived from the 2,2′-tethered binaphthyl structures and rigid and robust ladder backbones.

The helical ladder polymers exhibited a bright blue photoluminescence (PL) in chloroform under UV irradiation due to their fully π-conjugated backbone structures (Figure 6d), among which poly-**5S^{C1}** showed an excellent PL property with the higher fluorescence quantum yield (Φ_F) of 28% than those of poly-**7S^{C2}** (13%) and poly-**9S^{C3}** (15%). Because the Φ_F values of the precursor polymers (poly-**4S^{C1}**, poly-**6S^{C2}**, and poly-**8S^{C3}**) (Figure S20) and the previously reported 2,2′-alkylenedioxy-tethered 1,1′-binaphthyl-based molecules[11d,13f] varied only slightly with

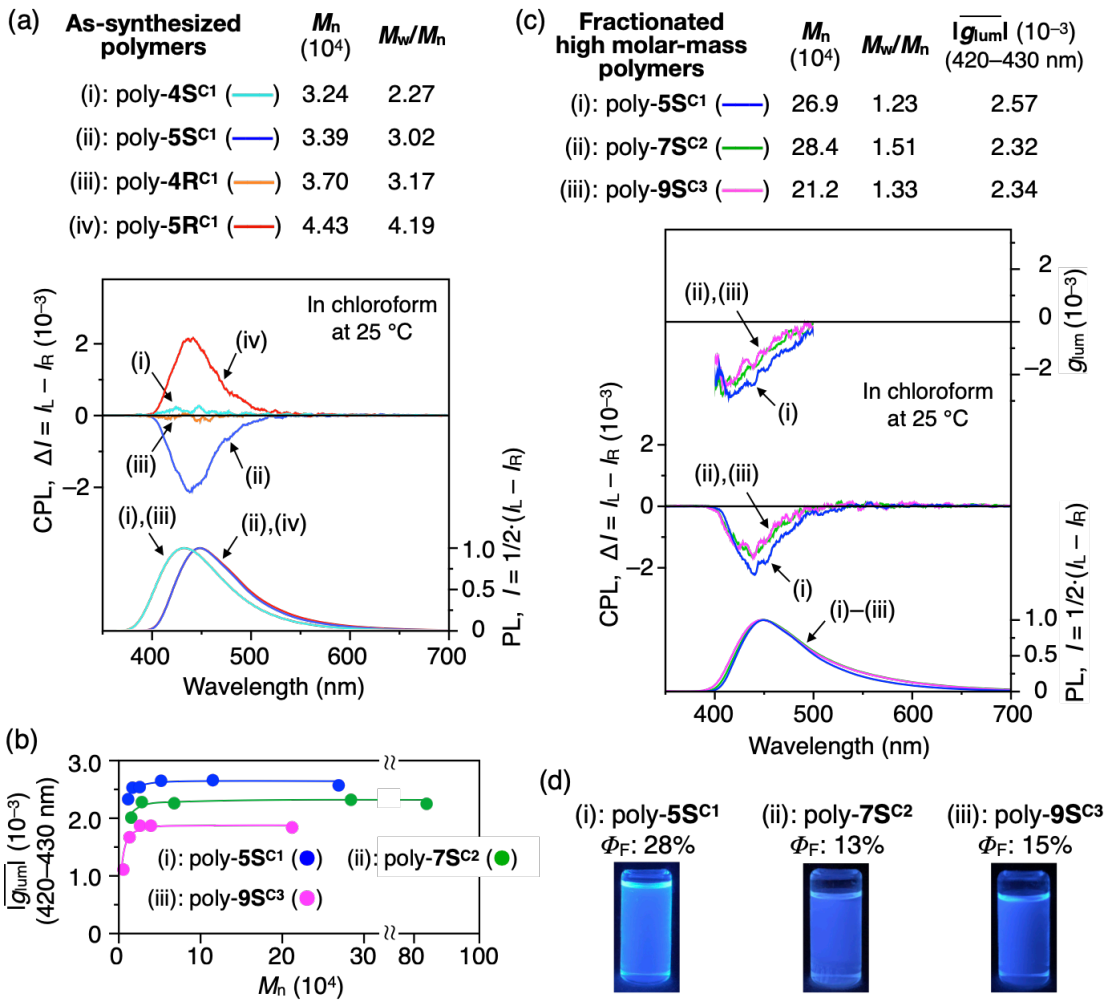

Figure 6. (a) CPL and normalized PL spectra of poly-**4S**^{C1} (i), poly-**5S**^{C1} (ii), poly-**4R**^{C1} (iii), and poly-**5R**^{C1} (iv) in chloroform at 25 °C. [Repeating units of polymer] = 0.10 mM. (b) Plots of luminescence dissymmetry factors ($|\overline{g_{lum}}|$) of poly-**5S**^{C1} (i), poly-**7S**^{C2} (ii), and poly-**9S**^{C3} (iii), which are estimated as average values in the range of 420–430 nm due to the relatively large wavelength-dependent variation, versus the M_n value. The g_{lum} values are defined as $2(I_L - I_R)/(I_L + I_R)$, where I_L and I_R are the PL intensities of the left- and right-handed circularly polarized light, respectively. For the SEC fractionation and the corresponding CPL spectra, see b and d in Figures S15–S17. (c) Normalized PL (bottom), CPL (middle), and g_{lum} (top) spectra of fractionated high molar-mass poly-**5S**^{C1} (i; **f1** in Figure S15b), poly-**7S**^{C2} (ii; **f2** in Figure S16b), and poly-**9S**^{C3} (iii; **f1** in Figure S17b) ($M_n > 20 \times 10^4$) measured in chloroform at 25 °C after SEC fractionation. λ_{ex} = 300 nm. (d) Photographs of poly-**5S**^{C1} (i), poly-**7S**^{C2} (ii), and poly-**9S**^{C3} (iii) in chloroform with 365-nm irradiation. Fluorescence quantum yields (Φ_F) are also shown.

the tether length, such a significant Φ_F change would be primarily relevant to a difference in the secondary structures rather than the local structure of the repeating unit.

The as-synthesized helical ladder polymers showed clear CPL signals (Figures 6a(ii,iv) and S13d(ii,iv)), while almost no or a very weak CPL was observed for the precursor polymers (Figures 6a(i,iii) and S13d(i,iii)) as well as the one-handed twisted ladder-type model molecules ((*S*)- and (*R*)-**3**^{C1}) (Figure S18b(ii,iv)),[21] clearly indicating that the regular helical arrangement of the polycyclic aromatic chromophores along the rigid one-handed helical ladder scaffolds plays a crucial role in the expression of CPL. At sufficiently high molar masses, poly-**5S**^{C1} showed a more intense CPL than poly-**7S**^{C2} and poly-**9S**^{C3}, and its luminescence dissymmetry factor ($|\overline{g_{lum}}|$), estimated as an average value in the range of 420–430 nm, reached ca. 2.6 × 10^{-3} (Figure 6b,c). The relatively higher $|\overline{g_{lum}}|$ value of poly-**5S**^{C1} was reproduced by the time-dependent-density functional theory (TD-DFT) calculations of the corresponding (*M*)-handed helical oligomer models (entries 2–4 in Table S3). The precise secondary structure modulation by tuning the binaphthyl dihedral angles in the repeating unit resulted in variation of the magnitudes and arrangement of the intrinsic magnetic and electric transition dipole moments, thereby leading to the optimization of the CPL performance. Considering its high Φ_F and $|g_{lum}|$ values, poly-**5**^{C1} is the most promising CPL material among all the reported one-handed helical ladder polymers synthesized by the alkyne benzannulations.[18-19,22]

Conclusion

We have succeeded in the first defect-free synthesis of the 2,2′-tethered binaphthyl-embedded helical ladder polymers, which could not be achieved in the previous attempt[14] using the conventional alkyne benzannulation due to its poor cyclization chemoselectivity. We found that the modified alkyne

benzannulation of the 6,6´-linked-1,1´-binaphthyl framework proceeded in a quantitative and perfect chemoselective manner due to the 2,6-dimethyl substituents introduced on the 4-alkoxyphenyl pendants, which completely suppressed any undesired reaction pathways, yielding a series of 2,2´-tethered binaphthyl-embedded regular one-handed helical ladder polymers with different tether lengths. The well-defined rigid and stable helical ladder structures provided the significantly strong CD signals, more than 6-fold higher than that of the corresponding 2,6-dimethyl-lacking polymer with structural defects. In addition, the fine-tuning of the helical geometries of the helical ladder polymers was achieved based on the rational control of the binaphthyl dihedral angles by the replacement of the tethering groups, leading to the strong CPL with the high Φ_F (28%) and $|\overline{g_{lum}}|$ (2.6×10^{-3}) values. We believe that the present approach to the precise macromolecular helix construction, which combines the defect-free ladderization with the simple tether replacement, can be further applied to the rational design and targeted synthesis of even more diverse and complicated secondary structures, leading to the emergence of advanced functions related to enantioselective catalysis and chiral recognition found in biological systems.

Acknowledgements

This work was supported in part by Grant-in-Aid for Specially Promoted Research (no. 18H05209 (E.Y. and T.I.)), Grant-in-Aid for Scientific Research (B) (no. 21H01984 (T.I.)), Grant-in-Aid for Challenging Research (Exploratory) (no. 23K17939 (T.I.)), and JST PRESTO (no. JPMJPR21A1 (T.I.)).

Keywords: alkyne benzannulations • helical polymers • ladder polymers • tethered binaphthyls • secondary structures

[1] a) L. Pu, *Chem. Rev.* **1998**, *98*, 2405–2494; b) S. G. Telfer, R. Kuroda, *Coord. Chem. Rev.* **2003**, *242*, 33–46; c) J. M. Brunel, *Chem. Rev.* **2007**, *107*, PR1-PR45; d) A. Shockravi, A. Javadi, E. Abouzari-Lotf, *RSC Adv.* **2013**, *3*, 6717–6746; e) M. Caricato, A. K. Sharma, C. Coluccini, D. Pasini, *Nanoscale* **2014**, *6*, 7165–7174; f) M. Krajnc, J. Niemeyer, *Beilstein J. Org. Chem.* **2022**, *18*, 508–523.

[2] a) A. Miyashita, A. Yasuda, H. Takaya, K. Toriumi, T. Ito, T. Souchi, R. Noyori, *J. Am. Chem. Soc.* **1980**, *102*, 7932–7934; b) T. Hayashi, *Acc. Chem. Res.* **2000**, *33*, 354–362; c) P. Kočovský, Š. Vyskočil, M. Smrčina, *Chem. Rev.* **2003**, *103*, 3213–3246; d) Y. Chen, S. Yekta, A. K. Yudin, *Chem. Rev.* **2003**, *103*, 3155–3212; e) M. M. Pereira, M. J. F. Calvete, R. M. B. Carrilho, A. R. Abreu, *Chem. Soc. Rev.* **2013**, *42*, 6990–7027; f) M. Hatano, K. Ishihara, *Asian J. Org. Chem.* **2014**, *3*, 352–365; g) Q. Yue, B. Liu, G. Liao, B.-F. Shi, *ACS Catal.* **2022**, *12*, 9359–9396; h) H.-J. Lee, K. Maruoka, *Chem. Rec.* **2023**, *23*, e202200286; i) N. Brodt, J. Niemeyer, *Org. Chem. Front.* **2023**, *10*, 3080–3109.

[3] a) D. J. Cram, *Angew. Chem., Int. Ed. Engl.* **1988**, *27*, 1009–1020; b) S. J. Lee, W. Lin, *Acc. Chem. Res.* **2008**, *41*, 521–537; c) M. H. Hyun, *J. Chromatogr. A* **2016**, *1467*, 19–32; d) L. Pu, *Chem. Commun.* **2022**, *58*, 8038–8048.

[4] a) Y. Imai, *Chem. Lett.* **2021**, *50*, 1131–1141; b) M. Hasegawa, Y. Nojima, Y. Mazaki, *ChemPhotoChem* **2021**, *5*, 1042–1058.

[5] a) G. Gottarelli, M. Hibert, B. Samori, G. Solladié, G. P. Spada, R. Zimmermann, *J. Am. Chem. Soc.* **1983**, *105*, 7318–7321; b) K. Akagi, *Chem. Rev.* **2009**, *109*, 5354–5401; c) Z.-g. Zheng, Y. Li, H. K. Bisoyi, L. Wang, T. J. Bunning, Q. Li, *Nature* **2016**, *531*, 352–356; d) T. Orlova, F. Lancia, C. Loussert, S. Iamsaard, N. Katsonis, E. Brasselet, *Nat. Nanotechnol.* **2018**, *13*, 304–308; e) S. Tokunaga, Y. Itoh, H. Tanaka, F. Araoka, T. Aida, *J. Am. Chem. Soc.* **2018**, *140*, 10946–10949; f) L. Qin, X. Liu, K. He, G. Yu, H. Yuan, M. Xu, F. Li, Y. Yu, *Nat. Commun.* **2021**, *12*, 699; g) Y. Chen, Y. Zhang, H. Li, Y. Li, W. Zheng, Y. Quan, Y. Cheng, *Adv. Mater.* **2022**, *34*, 2202309.

[6] a) I. Hanazaki, H. Akimoto, *J. Am. Chem. Soc.* **1972**, *94*, 4102–4106; b) S. F. Mason, R. H. Seal, D. R. Roberts, *Tetrahedron* **1974**, *30*, 1671–1682; c) L. Di Bari, G. Pescitelli, P. Salvadori, *J. Am. Chem. Soc.* **1999**, *121*, 7998–8004; d) M. Nishizaka, T. Mori, Y. Inoue, *J. Phys. Chem. A* **2011**, *115*, 5488–5495.

[7] a) C. Niezborala, F. Hache, *J. Am. Chem. Soc.* **2008**, *130*, 12783–12786; b) H. Zhang, X. Zheng, R. T. K. Kwok, J. Wang, N. L. C. Leung, L. Shi, J. Z. Sun, Z. Tang, J. W. Y. Lam, A. Qin, B. Z. Tang, *Nat. Commun.* **2018**, *9*, 4961; c) K. Takaishi, K. Iwachido, T. Ema, *J. Am. Chem. Soc.* **2020**, *142*, 1774–1779; d) K. Takaishi, T. Matsumoto, M. Kawataka, T. Ema, *Angew. Chem., Int. Ed.* **2021**, *60*, 9968–9972.

[8] a) J. E. Simpson, G. H. Daub, F. N. Hayes, *J. Org. Chem.* **1973**, *38*, 1771; b) S.-M. Park, M. T. Paffett, G. H. Daub, *J. Am. Chem. Soc.* **1977**, *99*, 5393–5399.

[9] For leading examples of optically-active 2,2´-tethered binaphthyl derivatives, see: a) E. P. Kyba, G. W. Gokel, F. De Jong, K. Koga, L. R. Sousa, M. G. Siegel, L. Kaplan, G. D. Y. Sogah, D. J. Cram, *J. Org. Chem.* **1977**, *42*, 4173–4184; b) D. W. Armstrong, T. J. Ward, A. Czech, B. P. Czech, R. A. Bartsch, *J. Org. Chem.* **1985**, *50*, 5556–5559; c) H. J. Deussen, E. Hendrickx, C. Boutton, D. Krog, K. Clays, K. Bechgaard, A. Persoons, T. Bjørnholm, *J. Am. Chem. Soc.* **1996**, *118*, 6841–6852; d) H. T. Stock, R. M. Kellogg, *J. Org. Chem.* **1996**, *61*, 3093–3105; e) J.-W. Park, M. D. Ediger, M. M. Green, *J. Am. Chem. Soc.* **2001**, *123*, 49–56; f) L. L. Schafer, T. D. Tilley, *J. Am. Chem. Soc.* **2001**, *123*, 2683–2684; g) R. A. van Delden, T. Mecca, C. Rosini, B. L. Feringa, *Chem. - Eur. J.* **2004**, *10*, 61–70; h) K. Takaishi, M. Kawamoto, K. Tsubaki, *Org. Lett.* **2010**, *12*, 1832–1835; i) Y. Li, A. Urbas, Q. Li, *J. Am. Chem. Soc.* **2012**, *134*, 9573–9576; j) K. Takaishi, S. Hinoide, T. Matsumoto, T. Ema, *J. Am. Chem. Soc.* **2019**, *141*, 11852–11857; k) M. Hasegawa, C. Hasegawa, Y. Nagaya, K. Tsubaki, Y. Mazaki, *Chem. - Eur. J.* **2022**, *28*, e202202218; l) K. Takaishi, S. Murakami, F. Yoshinami, T. Ema, *Angew. Chem., Int. Ed.* **2022**, *61*, e202204609.

[10] a) Y. Wang, Y. Li, S. Liu, F. Li, C. Zhu, S. Li, Y. Cheng, *Macromolecules* **2016**, *49*, 5444–5451; b) M. Monga Mulunda, C. van Goethem, Z. Zhang, E. Nies, I. Vankelecom, G. Koeckelberghs, *Eur. Polym. J.* **2018**, *101*, 248–254; c) W. Dujardin, C. Van Goethem, Z. Zhang, R. Verbeke, M. Dickmann, W. Egger, E. Nies, I. Vankelecom, G. Koeckelberghs, *Eur. Polym. J.* **2019**, *114*, 134–143.

[11] a) C. Tétreau, D. Lavalette, D. Cabaret, N. Geraghty, Z. Welvart, *J. Phys. Chem.* **1983**, *87*, 3234–3239; b) C. Rosini, S. Superchi, H. W. I. Peerlings, E. W. Meijer, *Eur. J. Org. Chem.* **2000**, 61–71; c) M. Schmid, L. Martinez-Fernandez, D. Markovitsi, F. Santoro, F. Hache, R. Improta, P. Changenet, *J. Phys. Chem. Lett.* **2019**, *10*, 4089–4094; d) N. Zhao, W. Gao, M. Zhang, J. Yang, X. Zheng, Y. Li, R. Cui, W. Yin, N. Li, *Mater. Chem. Front.* **2019**, *3*, 1613–1618; e) Y. Nojima, M. Hasegawa, N. Hara, Y. Imai, Y. Mazaki, *Chem. - Eur. J.* **2021**, *27*, 5923–5929.

[12] R. Ning, H. Zhou, S.-X. Nie, Y.-F. Ao, D.-X. Wang, Q.-Q. Wang, *Angew. Chem., Int. Ed.* **2020**, *59*, 10894–10898.

[13] a) G. Solladie, G. Gottarelli, *Tetrahedron* **1987**, *43*, 1425–1437; b) M. M. Green, S. Zanella, H. Gu, T. Sato, G. Gottarelli, S. K. Jha, G. P. Spada, A. M. Schoevaars, B. Feringa, A. Teramoto, *J. Am. Chem. Soc.* **1998**, *120*, 9810–9817; c) G. Proni, G. P. Spada, P. Lustenberger, R. Welti, F. Diederich, *J. Org. Chem.* **2000**, *65*, 5522–5527; d) Y. Li, C. Xue, M. Wang, A. Urbas, Q. Li, *Angew. Chem., Int. Ed.* **2013**, *52*, 13703–13707; e) K. Kakisaka, H. Higuchi, Y. Okumura, H. Kikuchi, *Chem. Lett.* **2014**, *43*, 624–625; f) X. Zhang, Z. Xu, Y. Zhang, Y. Quan, Y. Cheng, *ACS Appl. Mater. Interfaces* **2021**, *13*, 55420–55427.

[14] H.-C. Zhang, L. Pu, *Macromolecules* **2004**, *37*, 2695–2702.

[15] a) L. Yu, M. Chen, L. R. Dalton, *Chem. Mater.* **1990**, *2*, 649–659; b) J. Lee, A. J. Kalin, T. Yuan, M. Al-Hashimi, L. Fang, *Chem. Sci.* **2017**, *8*, 2503–2521; c) Y. C. Teo, H. W. H. Lai, Y. Xia, *Chem. - Eur. J.* **2017**, *23*, 14101–14112; d) X. Y. Wang, A. Narita, K. Müllen, *Nat. Rev. Chem.* **2018**, *2*, 0100; e) S. Che, L. Fang, *Chem* **2020**, *6*, 2558–2590; f) A. Jolly, D. D. Miao, M. Daigle, J. F. Morin, *Angew. Chem., Int. Ed.* **2020**, *59*, 4624–4633; g) S. Liu, D. Xia, M. Baumgarten, *Chempluschem* **2021**, *86*, 36–48; h) J. Lee, *Asian J. Org. Chem.* **2023**, *12*, e202300104.

[16] a) M. B. Goldfinger, T. M. Swager, *J. Am. Chem. Soc.* **1994**, *116*, 7895–7896; b) M. B. Goldfinger, K. B. Crawford, T. M. Swager, *J. Am. Chem. Soc.* **1997**, *119*, 4578–4593.

[17] T. Ikai, T. Yoshida, K. Shinohara, T. Taniguchi, Y. Wada, T. M. Swager, *J. Am. Chem. Soc.* **2019**, *141*, 4696–4703.

[18] W. Zheng, T. Ikai, E. Yashima, *Angew. Chem., Int. Ed.* **2021**, *60*, 11294–11299.

[19] a) W. Zheng, K. Oki, R. Saha, Y. Hijikata, E. Yashima, T. Ikai, *Angew. Chem., Int. Ed.* **2023**, *62*, e202218297; b) T. Ikai, A. Tanaka, T. Shiotani, K. Oki, E. Yashima, *Org. Mater.* **2023**, *5*, 184–190.

[20] a) M. M. Green, J. W. Park, T. Sato, A. Teramoto, S. Lifson, R. L. B. Selinger, J. V. Selinger, *Angew. Chem., Int. Ed.* **1999**, *38*, 3139–3154; b) T. Nakano, Y. Okamoto, *Chem. Rev.* **2001**, *101*, 4013–4038; c) E. Yashima, K. Maeda, H. Iida, Y. Furusho, K. Nagai, *Chem. Rev.* **2009**, *109*, 6102–6211; d) E. Schwartz, M. Koepf, H. J. Kitto, R. J. M. Nolte, A. E. Rowan, *Polym. Chem.* **2011**, *2*, 33–47; e) M. Fujiki, *Symmetry* **2014**, *6*, 677–703; f) F. Freire, E. Quiñoá, R. Riguera, *Chem. Rev.* **2016**, *116*, 1242–1271; g) E. Yashima, N. Ousaka, D. Taura, K. Shimomura, T. Ikai, K. Maeda, *Chem. Rev.* **2016**, *116*, 13752–13990; h) J. C. Worch, H. Prydderch, S. Jimaja, P. Bexis, M. L. Becker, A. P. Dove, *Nat. Rev. Chem.* **2019**, *3*, 514–535; i) T. Leigh, P. Fernandez-Trillo, *Nat. Rev. Chem.* **2020**, *4*, 291–310; j) Q. Wang, Y.-Q. Liu, R.-T. Gao, Z.-Q. Wu, *J. Polym. Sci.* **2023**, *61*, 189–196.

[21] Based on the TD-DFT calculations, weak CPL signals of (*S*)- and (*R*)-**3**$^{\mathbf{C1}}$ are most likely due to an unfavorable nearly orthogonal arrangement of the magnetic (*m*) and electric (*μ*) transition dipole moments ($\theta_{\mu,m}$ = 91.6°; $\cos\theta_{\mu,m}$ = –0.029) (entry 1 in Table S3).

[22] Meskers and co-workers reported the helical spiro-conjugated ladder polymers with the $|g_{lum}|$ values of ca. 4 × 10^{-3}, but their detailed structural characterization has not been performed, see: R. Ammenhäuser, P. Klein, E. Schmid, S. Streicher, J. Vogelsang, C. W. Lehmann, J. M. Lupton, S. C. J. Meskers, U. Scherf, *Angew. Chem., Int. Ed.* **2023**, *62*, e202211946.